

**M Barisonzi**

*on behalf of the ATLAS Collaboration*

Bergische Universität Wuppertal, Fachbereich C – Physik, Gaußstraße 20, D-42119 Wuppertal, Germany

E-mail: `marcello.barisonzi@physik.uni-wuppertal.de`

# QCD and Top physics studies in proton-proton collisions at 7 TeV centre-of-mass energy with the ATLAS detector

**Abstract.** Beginning from 2010, ATLAS collected proton-proton collision data at a centre-of-mass energy of 7 TeV, accumulating by the Spring of 2011 an integrated luminosity of  $\sim 200 \text{ pb}^{-1}$ . The high energy gives the possibility to produce a sizeable amount of top quarks, allowing for measurements of top quark properties and searches for heavy exotic resonances decaying to top-antitop pairs. Measurements of jet cross-sections confirm the predictions of perturbative QCD at the high energy of the Large Hadron Collider.

## 1. Introduction

The Large Hadron Collider (LHC) reached in 2010 the record centre-of-mass energy of  $\sqrt{s} = 7 \text{ TeV}$ , inaugurating the phase of physics studies at the TeV scale, with the possibility of solving outstanding issues of the Standard Model — such as the mechanism of Electroweak Symmetry Breaking or the origin of Dark Matter and Dark Energy — but also of finding new physics phenomena beyond the Standard Model itself. Before such studies can be accomplished, however, it is important to test the validity of the theoretical predictions and the simulation tools at the TeV scale. Section 2 describes the studies on the predictions of Next-to-Leading-Order perturbative QCD (NLO pQCD) models applied to the measurement of inclusive jet and dijet cross-sections.

Another important sector of physics studies at the LHC is top physics. The high beam energy and luminosity make the LHC a top factory, with  $\sim 13000 \text{ } t\bar{t}$  pairs created daily at a luminosity of  $10^{33} \text{ cm}^{-2} \text{ s}^{-1}$ . The large amount of statistics will facilitate precision measurements of the top quark that may help to explain the role that a particle of such a large mass plays in Electroweak Symmetry Breaking mechanisms — if any of these mechanisms is found. The measurements of the top quark cross-sections for the QCD and Electroweak production processes at ATLAS are presented in Section 3, which also contains a search for heavy resonances decaying to a  $t\bar{t}$  pair.

## 2. Jet cross-section measurements

The aim of these studies is to compare the NLO pQCD predictions for inclusive jets and dijet production. Inclusive single-jet double-differential cross sections are measured as a function of jet transverse momentum  $p_T$  and pseudorapidity  $y$ , while the dijet double-differential cross



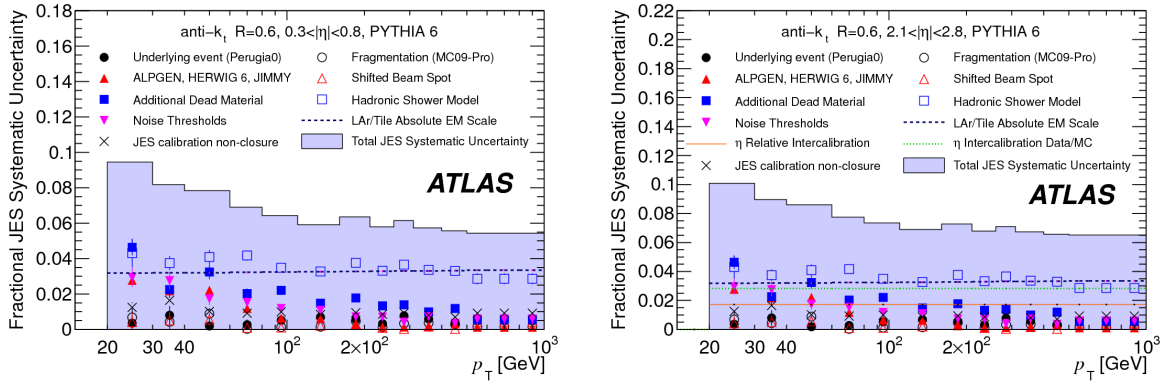


**Figure 1.** Fractional jet energy scale systematic uncertainty as a function of  $p_T$  for jets in the pseudorapidity region  $0.3 < |\eta| < 0.8$  (left) and  $2.1 < |\eta| < 2.8$  (right) [1].

section is measured as a function of the invariant mass of the dijet system,  $m_{12}$ , binned in the maximum rapidity of the two leading jets,  $|y|_{max} = \max(|y_1|, |y_2|)$  [1].

The cross section measurements are performed using jets reconstructed with the anti- $k_T$  algorithm [2]. For the inclusive jet measurements, jets are required to have  $p_T > 20$  GeV and be within  $|y| < 4.4$ . For the dijet mass measurements, the selection requires a leading jet with  $p_T > 30$  GeV and  $|y| < 4.4$ , and at least one sub-leading jet with  $p_T > 20$  GeV and  $|y| < 4.4$  [3]. The energy of the reconstructed jets is calibrated to obtain the energy of the Monte Carlo particle jets; the calibration of the Jet Energy Scale (JES) is in fact the largest factor contributing to systematic uncertainties, and can be affected by the following effects [1]:

- material and geometrical modelling of the detector;
- noise thresholds in the calorimeter;
- electromagnetic response of the calorimeter;
- beamspot position.

The jets unfolded to particle level are compared to the NLO pQCD prediction, calculated using the NLOJET++ 4.1.2 program [4] along with the CTEQ 6.6 NLO parton distribution functions [5]. The fixed-order NLO matrix element predictions are combined with a leading-log showering and fragmentation model — PYTHIA with LHC-specific tuning — to better describe the data. This introduces additional uncertainties in the JES estimation, due to [1]:

- hadronic shower modelling;
- event generator model;
- modelling of pile-up effects;
- effect of decorrelated JES uncertainty on dijet observables.

All JES uncertainties are added in quadrature; any deviation from unity of the closure test for JES corrections is treated as a fully correlated uncertainty and added linearly. The total uncertainty is estimated to be below 10% in the jet  $p_T$  range 20-1000 GeV (see Figure 1).

The double-differential inclusive jet cross-section, binned as a function of jet  $p_T$  and  $|y|$ , is shown in Figure 2. The ratio between the measured data and the theoretical predictions is compatible with unity, within the systematic and theoretical uncertainties.

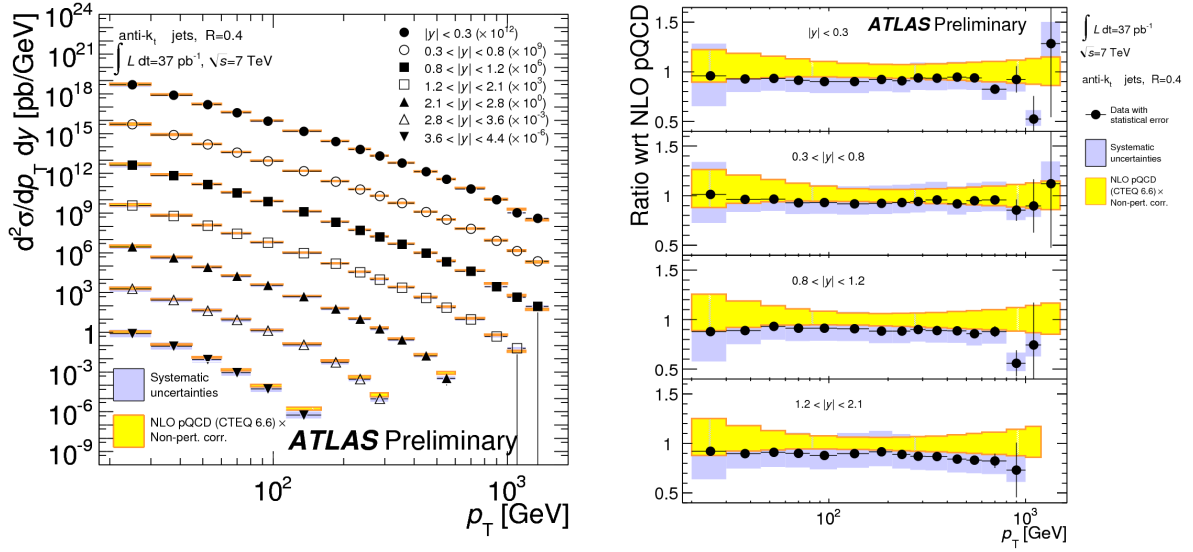


**Figure 2.** Left: inclusive jet double-differential cross-section as a function of jet  $p_T$  in different regions of  $|y|$  for jets identified using the anti- $k_T$  algorithm with  $R = 0.4$ . Right: ratio of the data to the theoretical prediction, with total systematic uncertainties on the theory and measurement [3].

The double-differential dijet cross-section, binned as a function of dijet mass and maximum jet rapidity  $|y|_{max}$ , is shown in Figure 3. Again, the ratio between the measured data and the theoretical predictions does not present any significant deviation from unity.

The good agreement between the NLO pQCD predictions and the data allows to search for the presence of resonances decaying into quark pairs. With 2010 data, the following resonant processes are searched for [6]:

- excited quarks;
- axigluons;
- Quantum Black Holes (QBH);
- Randall-Sundrum gravitons;
- quark contact interactions.

The study does not find any significant localized excess in the dijet mass spectrum (see Figure 4). Therefore, the following 95% CL limits can be set [6; 7]:

- excited quarks with masses in the interval  $0.80 < m_q < 2.49$  TeV are excluded;
- axigluons with masses in the interval  $0.80 < m < 2.67$  TeV are excluded;
- assuming six extra dimensions, Quantum Black Hole models with quantum gravity mass scale  $0.75 < M_D < 3.67$  TeV are excluded;
- quark contact interactions with a scale  $\Lambda < 9.5$  TeV are excluded.

No limits can be placed on Randall-Sundrum gravitons yet.

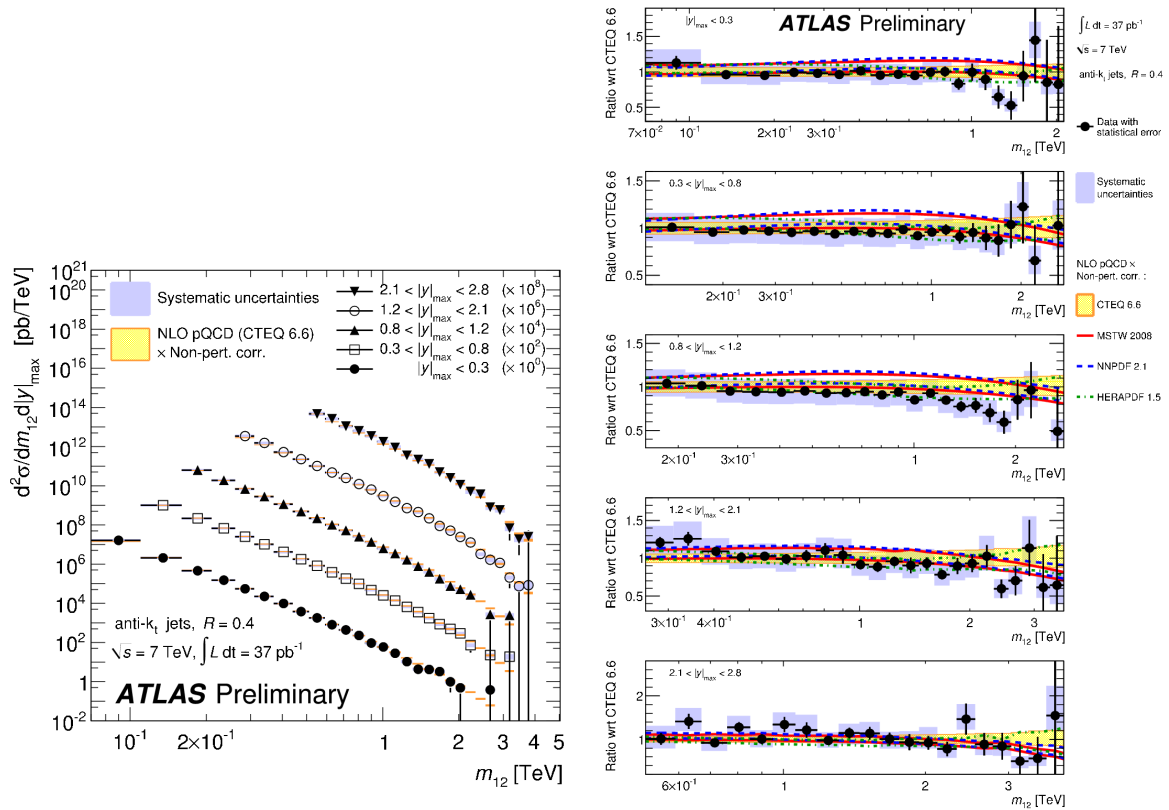


**Figure 3.** Left: dijet double-differential cross-section as a function of dijet mass, binned in the maximum rapidity of the two leading jets  $|y|_{\max}$ . The results are shown for jets identified using the anti- $k_T$  algorithm with  $R = 0.4$ . Right: the data points and the error bands are normalized to the theoretical predictions obtained by using the CTEQ 6.6 PDF set. The theoretical error bands obtained by using different PDF sets (MSTW 2008, NNPDF 2.1, HERAPDF 1.5) are also shown [3].

### 3. Top Physics

Top quark production at the LHC occurs mainly via two processes: top-antitop pair production from gluon-gluon fusion and single top electroweak production. Electroweak production can be broken down into three different subprocesses. Of these subprocesses, only the gluon-boson fusion (also known as t-channel) guarantees sufficient statistics and signal-to-background ratio to be studied with  $O(100 \text{ pb}^{-1})$  of data<sup>1</sup>.

Top quark events are characterised by a complex signature: the top quark decays almost exclusively to  $Wb$ , and the  $W$  boson can in turn decay to either quarks or leptons. The vast majority of top studies at ATLAS require the decay of at least one  $W$  boson into either  $(e, \nu)$  or  $(\mu, \nu)$ ; in the case of top pair production, events are classified as *semi-leptonic* or *di-leptonic* if, respectively, one or both  $W$  bosons decay leptonically. The selection of di-lepton events guarantees better purity at the cost of statistics, while semi-leptonic events offer a reasonable trade-off between event yield and background rejection.

All the top physics studies presented in this article implement a common selection:

<sup>1</sup> At Tevatron, the dominant production process was the s-channel quark-antiquark annihilation, which is negligible at LHC energies in 2011.

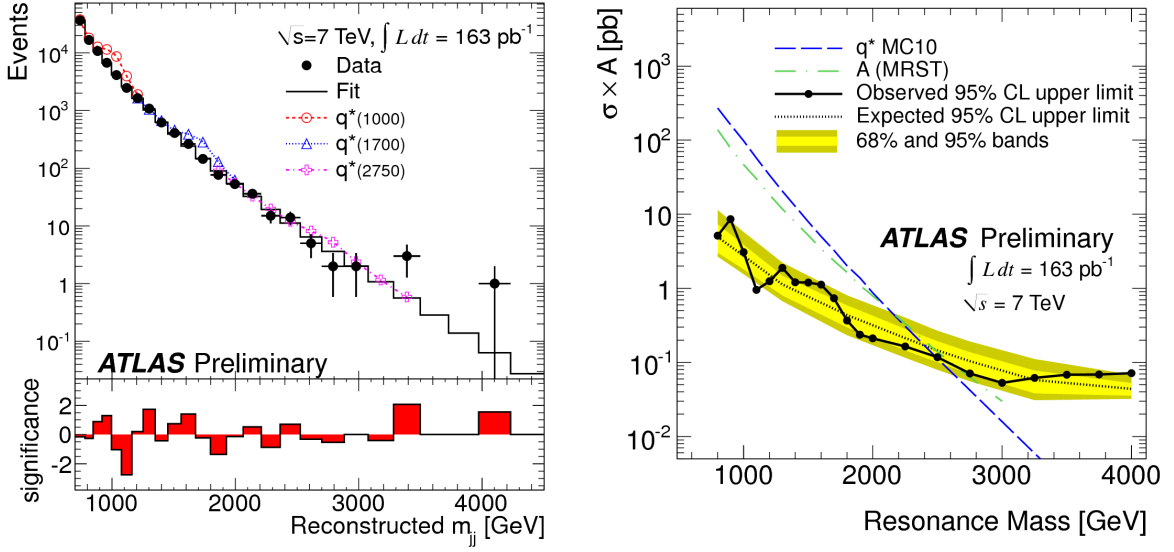


**Figure 4.** Left: the data dijet mass distribution with the predicted  $q^*$  signals for excited-quark masses of 1000, 1700, and 2750 GeV; for bins where the discrepancy has a Poisson  $p$ -value of less than 0.5, the bin-by-bin significance of the data-background difference is shown, in units of  $\sigma$ . Right: the 95% CL upper limit on  $\sigma \cdot \mathcal{A}$  (the product of the production cross-section and acceptance) as a function of dijet resonance mass [7].

- single lepton (electron or muon) trigger fired;
- at least one lepton (electron or muon) with  $p_T > 25$  GeV, lepton matched with the object firing the trigger<sup>2</sup>;
- jets with  $p_T > 25$  GeV; pair production studies require four or more central ( $|y| < 2.5$ ) jets, while single top studies require exactly two jets: one central and one forward ( $|y| > 2.5$ );
- at least one jet must be tagged as coming from a  $b$ -quark decay; the working point of the  $b$ -tagging algorithm is chosen to yield 50% tagging efficiency;
- missing transverse energy  $E_T^{\text{miss}} > 25$  GeV.

To further reduce the QCD multijet backgrounds, the reconstruction of a leptonically-decaying  $W$  boson is used in some studies, with the additional cut:  $E_T^{\text{miss}} + M_T(W) > 60$  GeV; where  $M_T(W)$  is the transverse mass of the reconstructed  $W$  boson [8; 9]. QCD background manifests itself as jets misidentified by the detector as leptons. Templates that model the behaviour of lepton-faking jets can be obtained from data; these templates require the presence of either a lepton failing some of the quality cuts or a jet with a large fraction of energy deposited in the electromagnetic calorimeter. A fit of the shape of the  $E_T^{\text{miss}}$  distribution from these events is then used to obtain the magnitude of the QCD background (see Figure 5).

### 3.1. Measurement of the $t\bar{t}$ cross-section

The measurement of the top quark pair production cross-section relies on a multivariate analysis. Additional methods, including cut-and-count methods and methods using fits to the kinematic distributions of the reconstructed top quark pairs were used as cross-check, but are not included in this article.

<sup>2</sup> The threshold for 2010 data was set to 20 GeV.

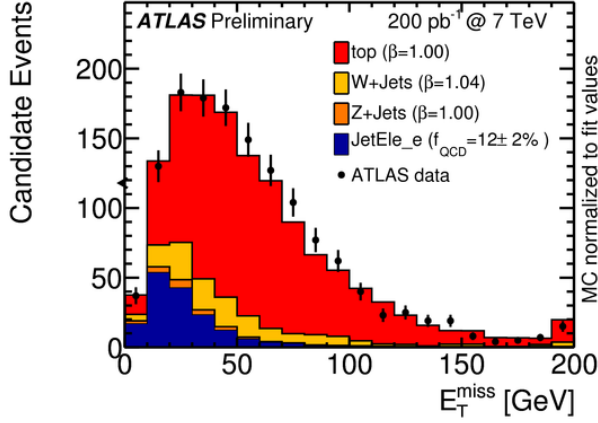


**Figure 5.** Fit of the  $E_T^{\text{miss}}$  distribution. The QCD template (blue) is obtained by selecting from data jets with an electromagnetic energy fraction between 0.8 and 0.95 [10], while the other templates are simulated using Monte Carlo generators [9].

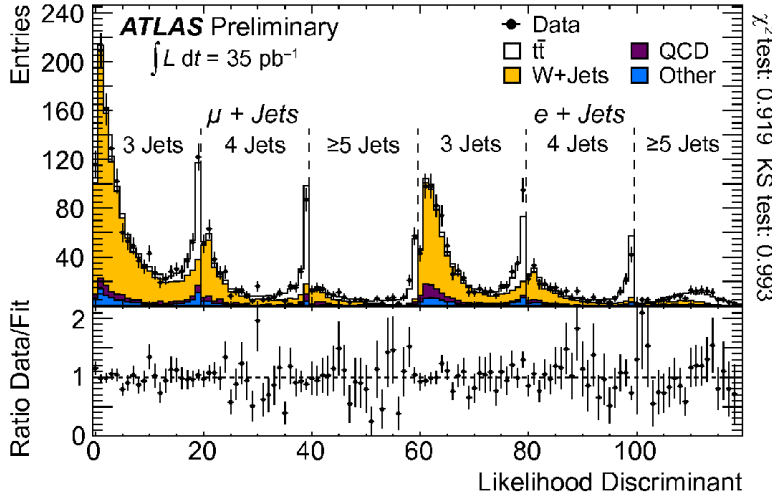


**Figure 6.** Fit of the likelihood discriminant  $D$  for the 3,4,5 jet bins in the semileptonic channels  $\mu$ +jets,  $e$ +jets [11].

The multivariate analysis constructs a likelihood discriminant  $D$  from four variables [11]:

- the pseudorapidity of the lepton;
- the aplanarity, defined as 1.5 times the smallest eigenvalue of the momentum tensor  $M_{ij} = \sum_{k=1}^{N_{\text{objects}}} p_{ik}p_{jk} / \sum_{k=1}^{N_{\text{objects}}} p_k^2$ , where  $p_{ik}$  is the  $i$ -th momentum component and  $p_k$  is the modulus of the momentum of object  $k$ ;
- the sum of the square of the transverse energy of all jets except the two leading ones, normalized to the sum of absolute values of all longitudinal momenta in the event;
- the average of the two lowest light-jet probabilities in the event, as computed by the  $b$ -tagging algorithm.

The discriminant  $D$  is fitted in the 3, 4 and 5 jet bins for both semileptonic channels  $e$ +jets and  $\mu$ +jets (see Figure 6). The fit yields a cross-section for  $t\bar{t}$  production of [11]:

$$\sigma_{t\bar{t}} = 186 \pm 10 \text{ (stat.) } {}^{+21}_{-20} \text{ (syst.) } \pm 6 \text{ (lumi.) pb.}$$

The results of the semileptonic and dilepton channels are combined by maximizing the likelihood as a function of  $\sigma_{t\bar{t}}$ , giving as a result [12]:

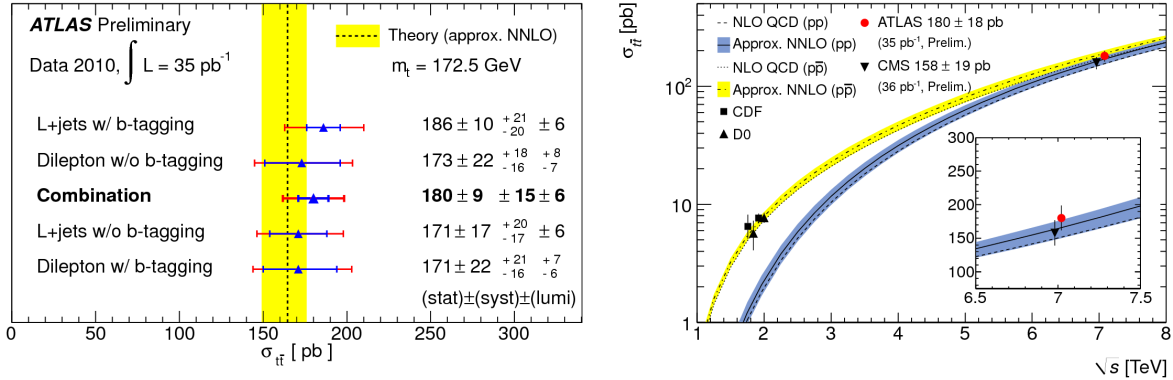


**Figure 7.** Left: the measured value of  $\sigma_{t\bar{t}}$  in the combined single-lepton and dilepton channels, including error bars for both statistical uncertainties only (blue) and with full systematics (red). The approximate NNLO prediction is shown as a vertical dotted line with its uncertainty. Right: measurements of  $\sigma_{t\bar{t}}$  from ATLAS and CMS in proton-proton collisions, and CDF and  $D\bar{O}$  in proton-antiproton collisions, compared to theoretical predictions assuming a top mass of 172.5 GeV as a function of  $\sqrt{s}$ . The presented result is indicated by the red circle [12].

$$\sigma_{t\bar{t}} = 180 \pm 9 \text{ (stat.)} \pm 15 \text{ (syst.)} \pm 6 \text{ (lumi.) pb.}$$

The result shows excellent agreement with a similar study from CMS [13] and with the extrapolation from the Tevatron measurements, and is consistent with the Standard Model predictions (see Figure 7).

### 3.2. Measurement of the single top cross-section

The measurement of the electroweak t-channel single top cross section is performed in the lepton+jets final state using two different techniques: a cut-and-count method and a neural network approach.

Both methods use a combination of selection variables that give good discrimination power against the underlying background processes. The most important variables are [8]:

1. the invariant mass of the  $b$ -tagged jet, the lepton and the neutrino,  $M_{l\nu b}$ ;
2. the pseudorapidity of the untagged jet,  $\eta(\text{l-jet})$ ;
3. the pseudorapidity of the  $b$ -tagged jet,  $\eta(\text{b-jet})$ ;
4. the scalar sum of the transverse energies of all jets  $H_T$ ;
5. the  $\Delta\eta$  distance between the  $b$ -tagged jet and the lepton,  $\Delta\eta(\text{b-jet}, \text{lepton})$ ;
6. the invariant mass of the two identified jets,  $M(\text{jet1}, \text{jet2})$ .

Variables 1-5 are used in the cut-and-count method. The neural network uses a combination of many more variables, where variables 1, 2 and 6 are the most important ones.

For the cut-and-count method, the measured cross-section and combined statistical and systematic uncertainty is [8]:

$$\sigma_t = 97_{-30}^{+54} \text{ pb.}$$

The measurement has a significance of  $6.1\sigma$  and the expected sensitivity is  $4.4\sigma$ .

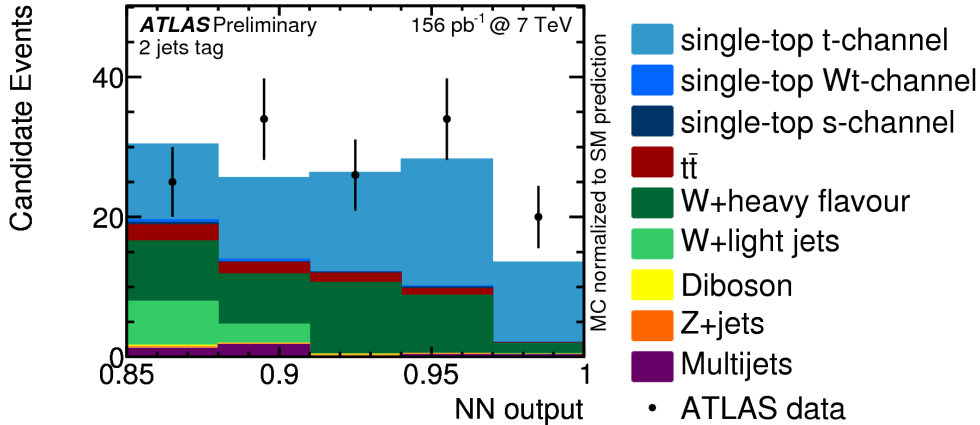


**Figure 8.** Neural network output distribution after the final selection cut normalized to number of expected events [8].

The neural network method gives a better sensitivity than the cut-and-count analysis. The output of the neural network for data and Monte Carlo is shown on Figure 8. The observed cross-section measurement and combined statistical and systematic uncertainty is [8]:

$$\sigma_t = 76_{-21}^{+41} \text{ pb.}$$

The measurement has a significance of  $6.2\sigma$  and the expected sensitivity is  $5.7\sigma$ .

### 3.3. Search for heavy resonances

The search for heavy resonances focuses on two benchmark processes that allow to estimate the experimental sensitivity in both the narrow- and wide-resonance regimes. As a narrow resonance, the top-colour  $Z'$  boson is chosen. In the leptophobic scenario, this resonance couples preferably to top quark pairs, with a resonance width of 1.2% of the  $Z'$  mass [9]. The model used for wide resonances is a Kaluza-Klein gluon  $g_{KK}$ , which appears in Randall-Sundrum (RS) models with a warped extra dimension; in this case, the resonance is predicted to be significantly wider than the detector and reconstruction algorithm's resolution [9].

As resonances are identified by excess data in the spectrum of the invariant mass of the  $t\bar{t}$  pair, mass resolution effects in the tail of the spectrum must be kept under control. The dominant source of these effects is the use of a jet from initial- or final-state radiation in the reconstruction of the invariant mass. To reduce this contribution, the  $dR_{min}$  algorithm selects the jets with  $p_T > 20$  GeV and  $|\eta| < 2.5$ , which also satisfy the condition  $\Delta R_{min} > 2.5 - 0.015 \times m_j$ , where  $m_j$  is the jet's mass and  $\Delta R_{min}$  is computed with respect to the closest lepton or surviving jet. The combination of three or four jets surviving the cuts enters in the top pair mass spectrum, allowing for merged jets or jets outside the acceptance [9]. The method is tested with Monte Carlo samples of  $Z'$  bosons, shown in Figure 9 (left).

The study searches for an excess of data in the reconstructed  $t\bar{t}$  mass spectrum, with respect to Standard Model predictions. As no statistically significant excess can be found in data (see Figure 9, right), the study sets the following 95% CL exclusion limits (see Figure 10):

- for narrow leptophobic  $Z'$  resonances, the maximum allowed cross-section ranges from 38 pb at  $m = 500$  GeV to 3.2 pb at  $m = 1300$  GeV;
- in Randall-Sundrum models, Kaluza-Klein gluons with masses below 650 GeV are excluded.



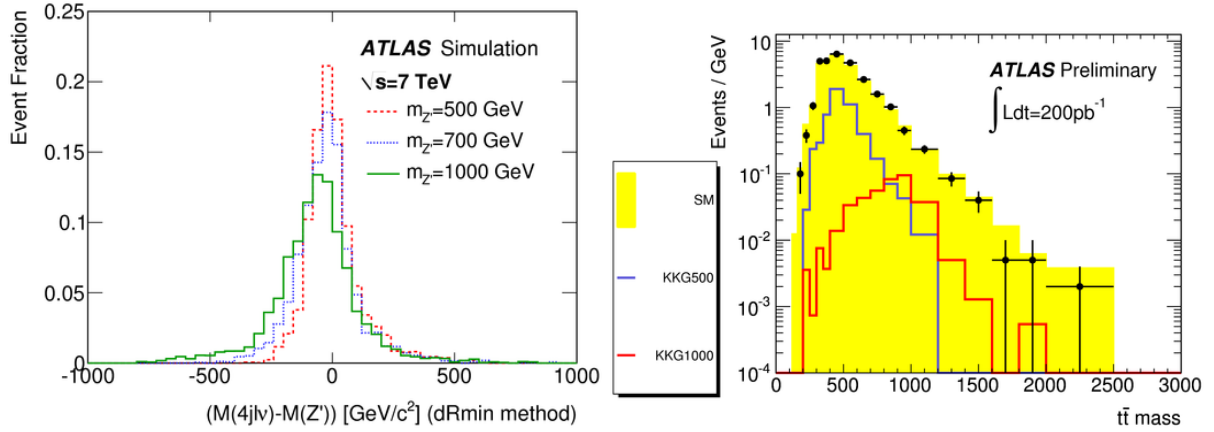


**Figure 9.** Left: reconstructed  $t\bar{t}$  pair invariant mass resolution (right) for three  $Z'$  boson masses:  $m_{Z'} = 500$  GeV,  $m_{Z'} = 700$  GeV and  $m_{Z'} = 1000$  GeV for the  $dRmin$  algorithm. Right:  $t\bar{t}$  mass spectrum reconstructed from data using the  $dRmin$  algorithm after selection cuts with expected Kaluza-Klein gluon spectrum for KK-gluon masses of 500 and 1000 GeV [9].

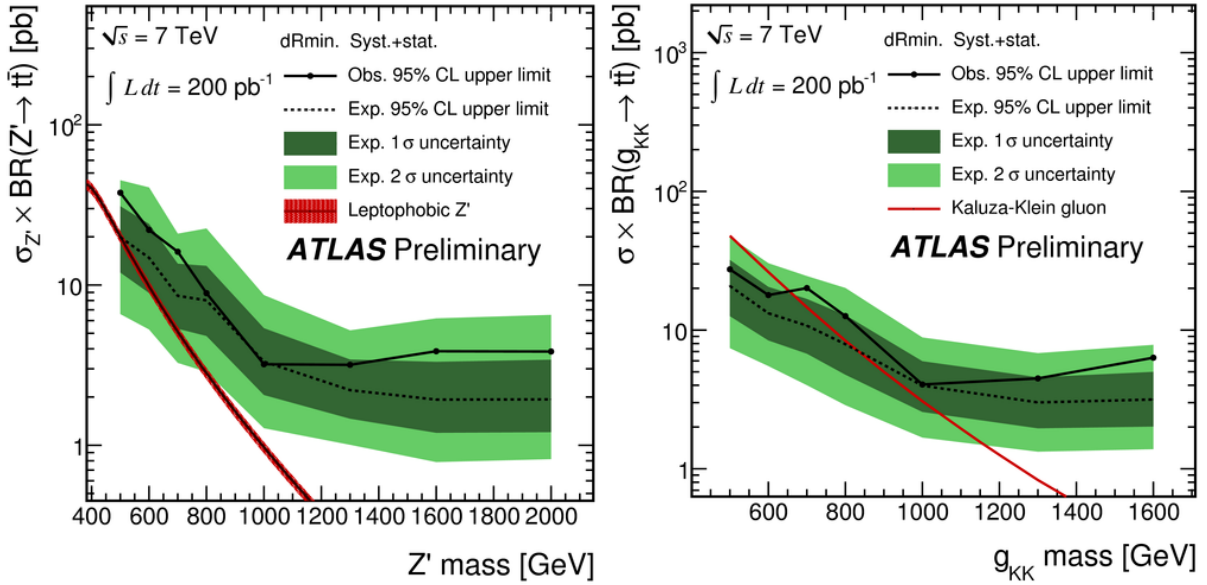


**Figure 10.** Expected (dashed line) and observed (black dots) upper limits on  $\sigma \times BR(Z' \rightarrow t\bar{t})$  (left) and  $\sigma \times BR(g_{KK} \rightarrow t\bar{t})$  (right) using the  $dRmin$  algorithm [9].

#### 4. Conclusions

The first year and a half of data taking at LHC allowed to study the Standard Model predictions at the unprecedented center of mass energy of 7 TeV. Next-to-Leading-Order Perturbative QCD predictions have been tested in the inclusive jet and dijet channels and show good agreement with data. No resonances were found in the dijet invariant mass spectrum.

In top physics, ATLAS made a first measurement of the  $t\bar{t}$  production cross-section, to compare against pQCD predictions at the new unprecedented LHC  $pp$  collision energy. The measurement confirms at this energy the good agreement — already observed at the lower energy of Tevatron — between data and theory on  $t\bar{t}$  production cross-section. Moreover, ATLAS measured with a level of significance of  $6.2\sigma$  the cross-section for the electroweak production of single top quarks in the t-channel, complementing the Tevatron measurement in the s-channel. The invariant mass spectrum of top quark pairs in  $t\bar{t}$  production was searched for the presence of both narrow and wide resonances; no resonance has been found yet.

#### References

- [1] The ATLAS Collaboration 2011 *The European Physical Journal C - Particles and Fields* **71**(2) 1–59
- [2] Cacciari M, Salam G P and Soyez G 2008 *JHEP* **0804** 063 (*Preprint* 0802.1189)
- [3] The ATLAS Collaboration 2011 Measurement of inclusive jet and dijet cross sections in proton-proton collision data at 7 TeV centre-of-mass energy using the ATLAS detector Tech. Rep. ATLAS-CONF-2011-047 CERN Geneva
- [4] Nagy Z 2003 *Phys. Rev.* **D68** 094002 (*Preprint* hep-ph/0307268)
- [5] Nadolsky P M *et al.* 2008 *Phys. Rev.* **D78** 013004 (*Preprint* 0802.0007)
- [6] The ATLAS Collaboration 2011 *New J. Phys.* **13** 053044. 51 p
- [7] The ATLAS Collaboration 2011 Update of the search for new physics in the dijet mass distribution in  $163 \text{ pb}^{-1}$  of  $pp$  collisions at  $\sqrt{s} = 7 \text{ TeV}$  measured with the ATLAS detector Tech. Rep. ATLAS-CONF-2011-081 CERN Geneva
- [8] The ATLAS Collaboration 2011 Observation of t channel single top-quark production in  $pp$  collisions at  $\sqrt{s} = 7 \text{ TeV}$  with the ATLAS detector Tech. Rep. ATLAS-CONF-2011-088 CERN Geneva
- [9] The ATLAS Collaboration 2011 A search for  $t\bar{t}$  resonances in the lepton plus jets channel in  $200 \text{ pb}^{-1}$  of  $pp$  collisions at  $\sqrt{s} = 7 \text{ TeV}$  Tech. Rep. ATLAS-CONF-2011-087 CERN Geneva
- [10] The ATLAS Collaboration 2011 Searches for single top-quark production with the ATLAS detector in  $pp$  collisions at  $\sqrt{s} = 7 \text{ TeV}$  Tech. Rep. ATLAS-CONF-2011-027 CERN Geneva
- [11] The ATLAS Collaboration 2011 Measurement of the top quark-pair cross-section with ATLAS in  $pp$  collisions at  $\sqrt{s} = 7 \text{ TeV}$  in the single-lepton channel using b-tagging Tech. Rep. ATLAS-CONF-2011-035 CERN Geneva
- [12] The ATLAS Collaboration 2011 A combined measurement of the top quark pair production cross-section using dilepton and single-lepton final states Tech. Rep. ATLAS-CONF-2011-040 CERN Geneva
- [13] The CMS Collaboration 2011 Combination of top pair production cross sections in  $pp$  collisions at 7 TeV and comparisons with theory Tech. Rep. CMS-PAS-TOP-11-001 CERN Geneva